ISSN 0027-1349, Moscow University Physics Bulletin, 2017, Vol. 72, No. 3, pp. 301–308. © Allerton Press, Inc., 2017.
Original Russian Text © A.V. Vershubskii, A.N. Tikhonov, 2017, published in Vestnik Moskovskogo Universiteta, Seriya 3: Fizika, Astronomiya, 2017, No. 3, pp. 83–90.

BIOPHYSICS AND MEDICAL PHYSICS

Electrons and Proton Transfer in Chloroplasts In Silico: 1. The Effect of Topological Factors on Energy Coupling in Chloroplasts with a Nonuniform Distribution of Protein Complexes

A. V. Vershubskii* and A. N. Tikhonov**

Department of Physics, Moscow State University, Moscow, 119991 Russia

**e-mail: vershoubskiy@mail.ru*

***e-mail: an_tikhonov@mail.ru*

Received August 31, 2016; in final form, November 15, 2016

Abstract—This paper presents a theoretical study of the effects of topological factors (density of thylakoid packing in grana) on the efficiency of energy coupling in chloroplasts. The study is based on a mathematical model of electron and proton transport processes coupled to ATP synthesis in chloroplasts. The model was developed by the authors earlier, and the nonuniform distribution of electron transport and ATP synthase complexes in the membranes of granal and intergranal thylakoids was taken into account in the model. The results of numerical experiments enabled the analysis of the distribution of lateral profiles of the transmembrane pH difference and the concentrations of mobile plastoquinone and plastocyanin electron transporters in granal and intergranal thylakoids and the dependence of this distribution on the metabolic state of class B chloroplasts (photosynthetic control state or the conditions of intensive ATP synthesis). Moreover, the influence of topological factors (the density of thylakoid packing in grana and the degree of thylakoid swelling) that affect the rate of diffusion of protons and mobile electron carriers in the intrathylakoid space and in the interthylakoidal gap was investigated. The results of numerical experiments that involved the variation of geometric parameters of the system revealed the influence of thylakoid thickness and the distance between the granal thylakoids on the lateral pH profiles inside the thylakoids (pH_i) and in the interthylakoidal gap (pH_o). Acidification of the intrathylakoid space characterized by the pH_i value increased concomitantly to the increase of the width of the interthylakoidal gap l_o and decreased concomitantly to the increase of the width of the intrathylakoidal space l_i.

Keywords: photosynthesis, electron and proton transport, mathematical modeling.

DOI: 10.3103/S0027134917030146

INTRODUCTION

Photosynthesis stands out among the large variety of biological processors, since it is a unique combination of photophysical, photochemical, and biochemical processes that involve energy transformation according to various mechanisms, such as absorption of light quanta by pigments of the light-harvesting antennas, energy migration to photoreaction centers, primary photochemical reactions, electron-transport processes, and numerous biochemical reactions of organic substance synthesis from atmospheric CO_2 and water [1, 2]. Functioning of the photosynthesis machinery is currently well characterized at various levels of structural and functional organization, including the level of individual enzyme systems and macromolecular complexes [3, 4]. The entire set of photosynthetic processes can be divided into two phases. The "light" phase of photosynthesis involves the breakage of chemical bonds in the primary electron donor molecule (water in the case of oxygenic systems) and the formation of ATP and NADPH. The energy of absorbed light quanta provides the energy demands of this phase. The subsequent "dark" phase involves the reduction of carbon dioxide to form sugars within the reducing pentose phosphate cycle [5, 6]. Energy accumulated in ATP and NADPH molecules is used during this phase.

Mathematical modeling of photosynthesis has been used for a long time and has laid the foundation for detailed quantitative analysis of feedback relationships in a branched network of intracellular metabolic processes and research on the regulatory mechanisms that provide the optimal functioning of the photosynthetic apparatus and its adaptation during the energy transformation processes inside a living cell [7–12]. However, quantitative description of bioenergetic processes in photosynthetic systems is complicated by a high degree of compartmentalization of the photosynthetic apparatus at different levels of structural organization. Nonuniform distribution of electron transport

and ATP synthase complexes in the thylakoid membranes is one of the puzzling features of the structural and functional organization of the photosynthetic apparatus in photosynthesizing organisms of the oxygenic type (cyanobacteria and chloroplasts of higher plants). This feature is especially distinct in the case of higher plant chloroplasts [13, 14]. Most of the complexes of photosystem 2 (PS2) are reportedly localized in the membranes of closely apposed granal thylakoids. In contrast to PS2, the complexes of photosystem 1 (PS1) and ATP synthase complexes are located in parts of the thylakoid membrane exposed to the stroma region (intergranal thylakoids and butt-ends of granal thylakoids). Cytochrome b_6f-complexes are distributed evenly between the granal and intergranal thylakoids [15].

Modeling of electron and proton transport processes with the complex structural features of chloroplasts taken into account can play an important role for the analysis of the influence of topological factors on the processes of energy coupling in chloroplasts. As often assumed [16, 17], functional and morphological heterogeneity of the lamellar system of the chloroplasts may be the reason for the difference between the pH values in the different compartments (for example, inside the granal and intergranal thylakoids). The heterogeneity of the thylakoids, along with their small size, is a considerable hindrance for the measurement of local pH values in different parts of the chloroplast. Therefore, mathematical modeling that takes the distinctive features of the spatial structure of the chloroplast into account can serve as one of the tools in the research on the influence of diffusion restrictions on the distribution of pH along the thylakoid membrane and the analysis of the effect of topological factors (spatial organization of thylakoids) on the rate of electron and proton transport and ATP synthesis in the chloroplasts.

Our earlier studies involved the construction of mathematical models that took key diffusion-controlled stages of noncyclic electron transport in class B chloroplasts into account, as well as the processes of transmembrane proton transfer into the thylakoids coupled to the above-mentioned processes [18–22]. The buffering properties of the thylakoid membrane were taken into account for the first time in these studies as the processes of transmembrane proton transfer into the thylakoids were analyzed. Moreover, the lateral heterogeneity of the lamellar system of the chloroplasts was taken into account as the diffusion-controlled stages of electron and proton transfer were described.

The present study summarizes the results of numerical experiments devoted to analysis of the influence of geometric parameters of the system (the degree of thylakoid compression in the grana and the size of the intrathylakoid space) on the spatially inhomogeneous distribution of pH and mobile electron transporters. Variation of geometric parameters of the system was shown to exert a significant effect on the acidification of the intrathylakoid space and the alkalization of the narrow interthylakoid gap and thus to affect the overall rate of electron transport in chloroplasts.

DESCRIPTION OF THE MODEL

Let us consider a mathematical model of electron transport in chloroplasts with a heterogeneous distribution of PS1 and PS2 complexes in the thylakoid membrane. This model also takes the transmembrane proton transfer and the processes of ATP synthesis into account. A chloroplast is considered a spatially inhomogeneous system with an uneven distribution of electron-transport complexes between the granal and intergranal thylakoids.

The Geometric Characteristics of the Thylakoid System of the Chloroplasts

The spatial arrangement of electron transport complexes in granal and intergranal thylakoids is schematically shown in Fig. 1. A flattened cylinder of the radius a is used to depict a granal thylakoid in the figure. An intergranal thylakoid is depicted by a wider cylinder of the radius b that extends into the stroma region beyond the granal thylakoid. The outer cylinder of the radius b includes a granal thylakoid (cylinder of the radius a) that forms a continuous structure with the intergranal thylakoid. The distance l_i between the internal surfaces of the thylakoid and the distance l_o between the adjacent thylakoids of the grana are the geometric parameters of the model.

Electron-Transport Processes

We have considered the processes of linear (noncyclic) transport of electrons from water to an external acceptor A_{ext} mediated by photosystem 1 (PS1) and photosystem 2 (PS2). We assume that the terminal acceptor A_{ext} is present in excess, because this is characteristic of isolated class B chloroplasts in the presence of an exogenous electron acceptor. The location of electron transport and ATP synthase complexes in the thylakoid membrane is shown in Fig. 1b. The distribution of PS1 and PS2 protein complexes among the granal and intergranal thylakoids is reportedly nonuniform [13, 23]. Our model uses the assumption that all PS2 complexes are located in the granal region A, and the PS1 complexes are located in the membranes of the intergranal thylakoids exposed to the stroma (region B). Cytochrome b_6f-complexes are uniformly distributed between regions A and B. Macromolecular protein complexes PS1, PS2, and b_6f are assumed immobile; thus, their position in the thylakoid membrane is fixed. Plastoquinone and plastocyanin, the mobile electron transporters that connect

PS2 to b_6f-complexes and theb_6f-complexes to PS1, respectively, can move in the lateral direction. The plastoquinone molecules (PQ) diffuse in the plane of the thylakoid membrane, whereas the molecules of plastocyanin (Pc) move in a relatively narrow gap of the intrathylakoid space (Fig. 1).

Mathematical description of electron-transport kinetics involved the following variables: $P^+_{700}(\mathbf{r}, t) \equiv [P^+_{700}]$ and $P^+_{680}(\mathbf{r}, t) \equiv [P^+_{680}]$ for the local concentrations of oxidized PS1 (P^+_{700}) and PS2 (P^+_{680}) reaction centers, respectively, $Pc(\mathbf{r}, t) \equiv [Pc]$, the local concentration of oxidized plastocyanin, and $Q(\mathbf{r}, t) \equiv [Q]$, the local concentration of oxidized plastoquinone. All these functions were defined as local concentrations of the corresponding components in a neighborhood of a point $\mathbf{r}$ at the time point t. A more detailed description of the model was given in [21, 22].

Proton Transport Processes

The variables $H_i(\mathbf{r}, t) \equiv [H^+_i]$ and $H_o(\mathbf{r}, t) \equiv [H^+_o]$ that correspond to the local concentrations of hydrogen ions inside a thylakoid and in the interthylakoid space of the grana were used to describe the proton transport processes. Hydrogen ions present in the system can diffuse in the aqueous phase of the intrathylakoid volume and in the narrow gap of the interthylakoid space of the grana. The model we developed addresses the processes that lead to a change in the activity of hydrogen ions in the interthylakoid gap and in the intrathylakoid space. Proton transport processes that take place outside the thylakoids include the uptake of protons from the interthylakoid gap coupled to plastoquinone reduction on the outer (acceptor) side of PS2 and the diffusion of protons from the stroma into the interthylakoid gap. The liberation of protons inside the thylakoids occurs due to light-induced decomposition of water in PS2 and due to the oxidation of plastoquinol (PQH_2) by the cytochrome b_6f-complex (Fig. 1). Release of protons from the thylakoids is taken into account along with proton transport into the thylakoids. The release of protons involves proton flux through the ATP synthase ($J^{ATP}_{H^+}(\mathbf{r})$) and passive leakage of protons through the thylakoid membrane ($J^{p}_{H^+}(\mathbf{r})$).

Hydrogen ions present in the system under consideration can diffuse in the aqueous phase of the intrathylakoid volume and in the narrow gap of the interthylakoid space of the grana (Fig. 1). The interaction of hydrogen ions with proton acceptor groups fixed on the inner and outer surfaces of the thylakoid membrane ($H^+ + M^- \leftrightarrow MH$) is taken into account in this case as well. The pH value in the stroma (pH_s) is assumed constant. The condition of $pH_s \approx$ const is fulfilled in the case of class B chloroplasts due to the high buffering capacity of the external environment and the chloroplasts themselves [21].

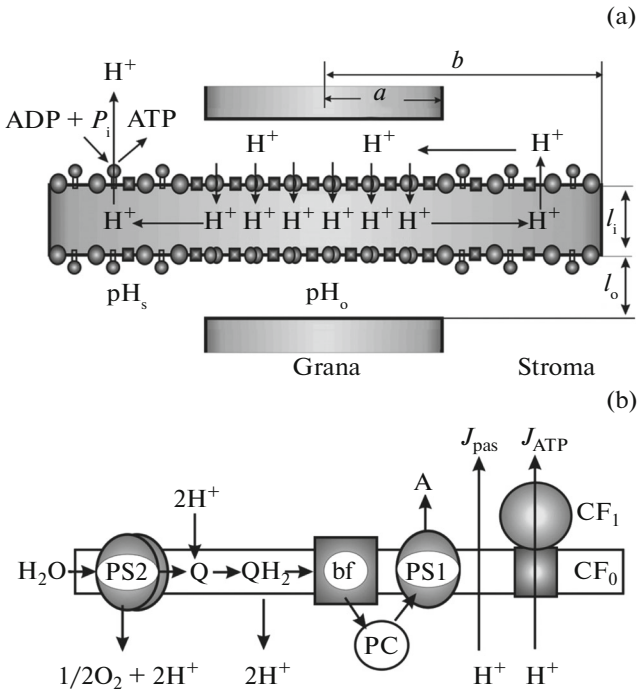

Fig. 1. The geometry of the thylakoid system simulated by the model and the pathways of proton transfer (a) and the electron transport chain considered within the model (b). The location of the electron transport and ATP synthase complexes of the thylakoid membrane considered within the model is shown schematically with the lateral heterogeneity of the thylakoids taken into account.

The function $J^{ATP}_{H^+}(\mathbf{r}, t)$ that described the proton flux through ATP synthase was defined by the following expression

$$J^{ATP}_{H^+}(r, t) = J_0 \frac{H_o(r,t)[10^{\Delta pH} - 1]}{\alpha + H_o(r,t)[10^{\Delta pH} + \beta]}. \qquad (1)$$

The choice of this expression for $J^{ATP}_{H^+}(r, t)$ was justified in [19, 21]. The variable $H_o(r, t) \equiv [H^+_s]$ in the equation (1) is constant and corresponds to the local concentration of hydrogen ions outside the thylakoid (in the stroma), and ΔpH is the transmembrane pH difference ($\Delta pH(r, t) = pH_s(r, t) - pH_i(r, t)$). The coefficients α and β in the equation (1) are determined by the pK_A value of the protonated group and by the ratio of the effective rate constants that characterize the functioning of ATP synthase (see [21] for details). If the function $J^{ATP}_{H^+}(r, t)$ is known, one can easily determine the total proton flux through the

ATP synthase and infer the rate of ATP formation from the former:

$$J_{\mathrm{ATP}}(t) = \frac{k_{\mathrm{ATP}}}{m} \cdot \frac{2\pi}{b^2 - a^2} \int_a^b J_{\mathrm{H}^+}^{\mathrm{ATP}}(r,t) r dr. \quad (2)$$

The coefficient k_{ATP} in the equation (2) is a parameter of the model that is determined by the number of active ATP synthase complexes located in the stromal part of the thylakoid membrane ($a \le r \le b$) and m is the stoichiometric coefficient (H^+/ATP).

The system of equations that describes the behavior of electron carriers and the changes of proton concentration inside the thylakoid $[H_i^+]$ and in the interthylakoid gap $[H_o^+]$ assumes the following form:

$$\frac{\partial [P_{680}^+(r,t)]}{\partial t} = L_2 \cdot k_{\mathrm{P680}} \cdot ([P_{680}]_0 - [P_{680}^+(r,t)]) \times [PQ(r,t)] \cdot [H_o^+(r,t)] - k_{\mathrm{H_2O}}[P_{680}^+(r,t)], \quad (3)$$

$$\frac{\partial [P_{700}^+(r,t)]}{\partial t} = L_1 \cdot k_{\mathrm{P700}} \cdot [A_{\mathrm{ext}}] \cdot ([P_{700}]_0 - [P_{700}^+(r,t)]) - k_{\mathrm{Pc}} \cdot ([Pc]_0 - [Pc(r,t)]) \cdot [P_{700}^+(r,t)], \quad (4)$$

$$\frac{\partial [Pc(r,t)]}{\partial t} = D_{Pc} \nabla^2 [Pc(r,t)] + k_{Pc}([Pc]_0 - [Pc(r,t)]) \cdot [P_{700}^+] - \sigma_{\mathrm{bf}} k_{\mathrm{Q}}([PQ(r,t)], [Pc(r,t)], [H_i^+(r,t)]), \quad (5)$$

$$\frac{\partial [PQ(r,t)]}{\partial t} = D_{\mathrm{PQ}} \nabla^2 [PQ(r,t)] - 0.5 \cdot L_2 \cdot k_{\mathrm{P680}} \times ([P_{680}]_0 - [P_{680}^+(r,t)]) \times ([\mathrm{PQ}(r,t)] \cdot [H_o^+(r,t)]) + \sigma_{\mathrm{bf}} k_{\mathrm{Q}}([PQ(r,t)], [Pc(r,t)], [H_i^+(r,t)]), \quad (6)$$

$$\left[1 + \frac{K_o B_o}{(K_o + [H_o^+])^2}\right] \frac{dH_o^+}{dt} = D_{H^+} \nabla^2 [H_o^+(r,t)] - \frac{2}{l_o} [Q][H_o^+]\{L_2 k_{\mathrm{P680}}([P_{680}]_0 - [P_{680}^+])\} - J_{H+}(t) - J_{ATP}(t), \quad (7)$$

$$\left[1 + \frac{K_i B_i}{(K_i + [\mathrm{H}_i^+])^2}\right] \frac{dH_i^+}{dt} = D_{H^+} \nabla^2 [H_i^+(r,t)] - \frac{2}{l_i} \{k_{\mathrm{H_2O}}[\mathrm{P}_{680}^+] + 2\sigma_{\mathrm{bf}} k_{\mathrm{Q}}([Q], [Pc], [H_i^+]) - J_{H+}(t) - J_{ATP}(t)\}. \quad (8)$$

The parameters L_1 and L_2 describe the number of light quanta that arrive to the reaction centers P_{700} and P_{680}, respectively, per unit time. The constant values with a 0 index are the maximal values of the respective variables. The constant σ_{bf} is the surface density of the b_6f-complexes in the membrane, and $k_{\mathrm{H_2O}}$, k_{P680}, k_{Q}, k_{Pc}, and k_{P700} are the effective rate constants of the reactions shown in Fig. 1. The set of model parameters K_i, K_o, B_i, and B_o ($i = 1, ..., n$) characterizes the buffer properties of the system. K_i and K_o are the equilibrium constants for the reaction of proton binding by the buffer groups located inside and outside of the membrane thylakoids, respectively, and B_i and B_o are the concentrations of these buffer groups (see [19] for details). Model parameters l_i and l_o characterize the linear dimensions of the intrathylakoid space and the interthylakoid gap.

The function $k_{\mathrm{Q}}\{[Q], [Pc], [H_i]\} = 1/\tau_{\mathrm{Q}}$ that we defined previously [19] is an effective rate constant that characterizes the set of processes associated with the oxidation of the plastoquinol molecule PQH_2. The characteristic time of plastoquinol oxidation τ_{Q} is determined by the rate of direct interaction of the molecule with the b_6f-complex and the time of electron transfer from the b_6f-complex to the plastocyanin molecule [19]. The rate of oxidation of PQH_2 depends on the concentration of hydrogen ions inside the thylakoids (for more details, see [19, 21]). The software developed by the authors earlier in collaboration with Priklonskii [18] was used to perform the calculations.

RESULTS AND DISCUSSION

Lateral pH Profiles

Lateral profiles of the pH inside the thylakoid (pH_i) and in a narrow gap between the granal thylakoids (pH_o) are shown in Fig. 2. These profiles were calculated for the metabolic states 3 and 4. The pH value in the stroma was not changed during the subsequent calculations and was assumed constant (pH_s = 8). The curves shown in the figure correspond to different values of the model parameters, namely, the width l_o of the interthylakoid gap and the width l_i, a characteristic of the dimensions of the intrathylakoid space. The effective diffusion coefficients of the protons D_{H} and those of the mobile electron carriers D_{PQ} and D_{Pc} were not changed during the calculations either. The initial pH values (prior to the illumination of the chloroplasts) inside the thylakoids and in the gap were the same as pH_s, that is, $pH_i(0, r) = pH_o(0, r) = 8$.

The profiles of intrathylakoid $pH_i(r)$ for the stationary states 3 and 4 differ markedly, as evident from Fig. 2. The decrease of pH within the thylakoid under the conditions of photosynthetic control (metabolic state 4) is more pronounced than the decrease of pH under the conditions of intense ATP synthesis (state 3) when protons are transported out of the thylakoids by the actively functioning ATP synthase complexes. A homogeneous profile of the intrathylakoid pH_i is

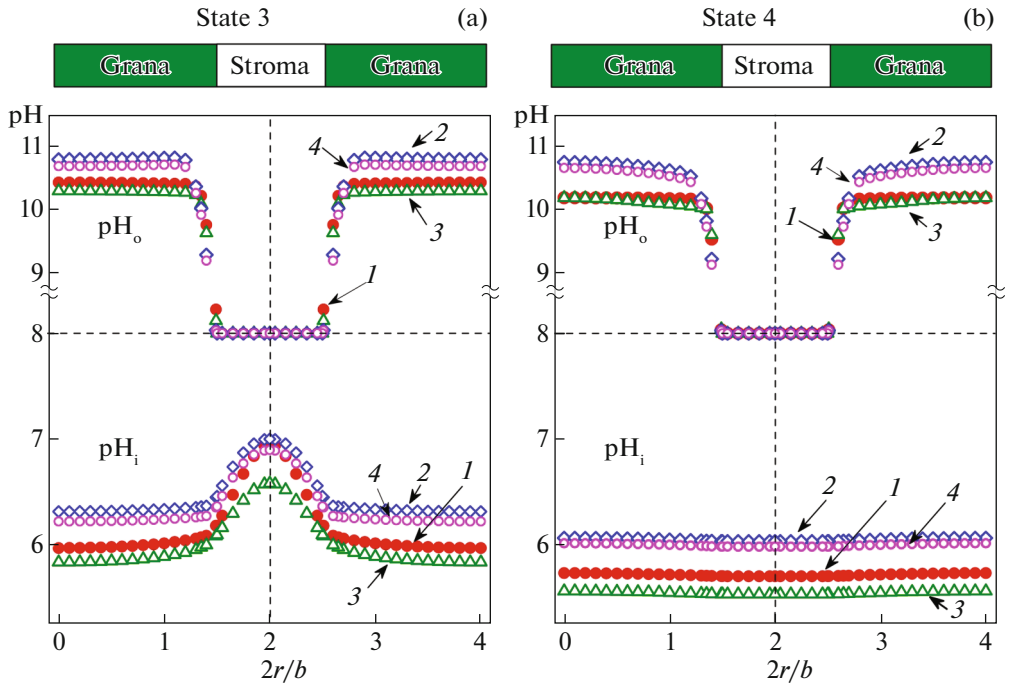

Fig. 2. Lateral pH profiles inside (pH_i) and outside (pH_o) of the thylakoid in the stationary states 3 (a) and 4 (b), calculated for different values of geometric parameters of the model (l_o and l_i). *1*, "reference" curve that corresponds to the l_o/l_i ratio of 0.1; *2*, after a tenfold increase of l_i; *3*, after a tenfold increase of l_o; *4*, after a tenfold increase of both l_o and l_i. The dimensionless variable $R = 2r/b$ characterizes the distance from the center of the grana.

characteristic of the state 4. However, the profile exhibits a considerable curvature near the border of the granal and intergranal regions in the state 3 due to additional flow of protons out of the thylakoids through the ATP synthase complexes located in the intergranal thylakoids. The outward flow of protons through the ATP synthase complexes is not compensated by the influx of protons from the granal area of the thylakoid due to decelerated lateral diffusion of protons. As a result, the decrease of pH_i in the granal area of the thylakoid is more pronounced than that in the stromal region of the intrathylakoid space that loses protons due to intensive outward flow of protons through the ATP synthase complexes.

Variation of the geometric dimensions of the thylakoids and the density of thylakoid packing in the grana exerts a noticeable effect on the lateral pH profiles. As evident from Fig. 2, pH_i decrease becomes more pronounced as the width l_o of the interthylakoid gap increases and less pronounced upon an increase of the width l_i of the intrathylakoid space (at a constant width of the gap). Interestingly, the character of the nonhomogeneous pH_i profile did not change in the state 3 (Fig. 2a), whereas the increase of the geometric dimensions led to an increase of the nonuniformity of the pH_i profile in state 4 (Fig. 2b).

The results of the calculations (Fig. 2) also showed that the illumination of chloroplasts led to a significant increase in pH_o in the gap between the thylakoids of the grana (pH ≈ 10.2–10.8, depending on the parameters of the model). The decrease in the activity of hydrogen ions in the interthylakoid gap is due to the rapid consumption of protons coupled to the reduction of plastoquinone on the acceptor site of PS2. The influx of protons from the stroma ($pH_s < pH_o$) is not sufficient for the timely compensation of the light-induced decrease of the proton concentration in the gap between the neighboring thylakoids of the grana. As the width of the interthylakoid gap l_o is increased (at l_i = const), the light-induced pH increase in the gap becomes less pronounced. This is due to an increase of the volume of the interthylakoid gap, from which the protons move towards the plastoquinone molecules that are reduced on the acceptor site of PS2. In contrast, an increase in the width of the intrathylakoid space l_i (at l_o = const) leads to an even more pronounced increase of pH in the gap. The latter effect is apparently due to weaker acidification of the intrathylakoid space that accounts for a less intensive passive leakage of protons from the intrathylakoid space into the gap. As evident from the calculations presented in this study, the light-induced pH increase in the gap is only weakly dependent on the functioning of ATP synthase complexes, although the alkalinization of the gap is somewhat more pronounced in state 3.

The effective diffusion rate of protons inside the thylakoids and in the intermembrane space is an additional factor that may affect the lateral profiles of

The effect of geometric parameters of the model on the rate of ATP synthesis (J_{ATP})

No.	Model parameters	J_{ATP} (arb. units)
1	$l_o^{st}/l_i^{st} = 0.1$ ("standard")	1
2	$l_i = 10 \times l_i^{st}$	0.95
3	$l_i = 10 \times l_o^{st}$	1.35
4	$l_i = 10 \times l_i^{st}$ $l_i = 10 \times l_o^{st}$	1.05

$pH_o(r)$ and $pH_i(r)$, since the acceleration of proton diffusion promotes a more rapid equalization of proton concentrations in the entire intrathylakoid volume. An increase of the velocity of lateral diffusion of protons in the interthylakoid gap, in its turn, promotes the acceleration of electron transport in chloroplasts and thus accelerates the functioning of "proton pumps" and provides a more pronounced decrease in pH within the thylakoids.

ATP Synthesis Rate

Variation of geometric parameters that affect the transthylakoid pH difference ($\Delta pH = pH_s - pH_i$) exerts an effect on the rate of ATP synthesis (J_{ATP} calculated according to the formulae (1–2)) as well. As shown in the table, an increase in the width of the interthylakoid gap (parameter l_o) has a considerable effect on the steady-state rate of ATP synthesis. This is apparently due to the increase of ΔpH at the stromal thylakoids where the ATP-synthase complexes are located (Fig. 2a) upon an increase in l_o. As we noted earlier [12, 21], this effect of l_o can be easily explained by the decrease in gap alkalization upon an increase in gap width. The decrease in alkalization accounts for a weaker effect of suppression of PS2 functioning. Deceleration of PS2 functioning upon the alkalization of the gap can be due to the suppression of the formation of protonated plastoquinol in PS2 ($PQ + H_o^+ \rightarrow PQH_2$) at high pH_o levels. Interestingly, an increase in the width of the intrathylakoid space (a tenfold increase of the parameter l_i) leads to an insignificant decrease in J_{ATP}: this is probably due to the inhibition of PS2 functioning due to a stronger alkalization of the interthylakoid gap.

Lateral Concentration Profiles of Mobile Electron Transporters

The stationary lateral profiles of oxidized plastoquinone ([*PQ*]) concentration calculated for metabolic states 3 and 4 are shown in Fig. 3a. As evident from Fig. 3, the lateral profiles [*PQ*(*r*)] for the stationary states 3 and 4 are similar, but the oxidation of *PQ* under the conditions of photosynthetic control is less intensive than under the conditions of intense ATP synthesis (compare the pair of curves *1*, *2*, and *3* in Fig. 3). Similarly to the previous case, the model predicted that an inhomogeneous [*PQ*] profile would be established in the chloroplasts, with the concentration

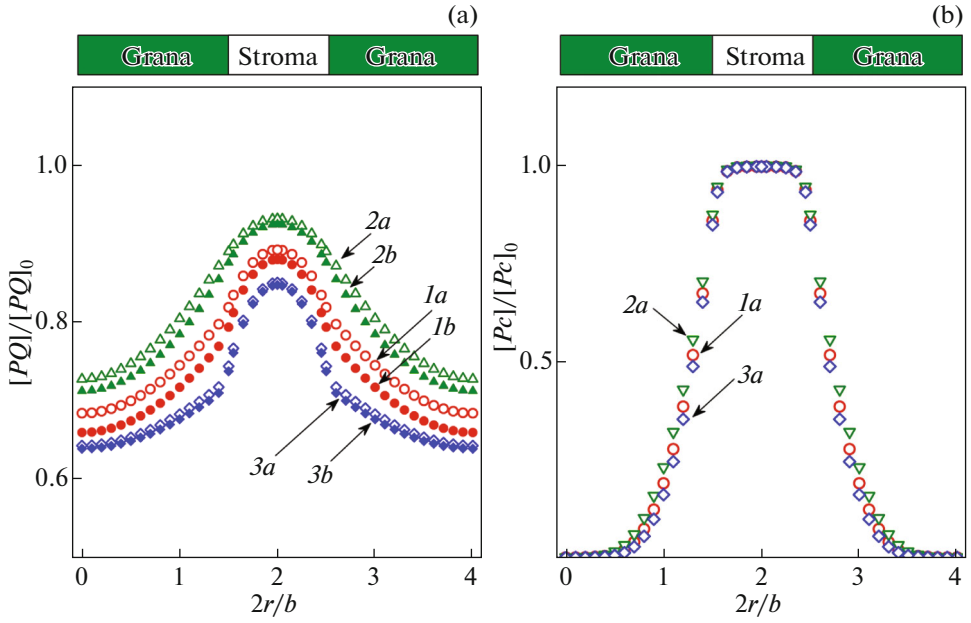

Fig. 3. Lateral concentration profiles for the oxidized form of (a) plastoquinone (*PQ*) and (b) plastocyanin (*Pc*) in stationary states 3 (curves *1a*, *2a*, and *3a*) and 4 (curves *1b*, *2b*, and *3b*) calculated for different values of the geometric parameters of the model (l_o and l_i). Curves *a* and *b* for plastocyanin are identical. The numbers of the curves correspond to those in Fig. 2.

of oxidized plastoquinone in the granal region of the thylakoid being lower than that in the stromal region. The increase of the width of the interthylakoid gap l_o (at l_i = const) leads to a decrease of the concentration of oxidized plastoquinone at every point of space. This is due to more intensive acidification of the interthylakoid space and the related reduction of the rate of plastoquinol (PQH_2) oxidation by the cytochrome b_6f-complex. Conversely, an increase of the width of the intrathylakoid space l_i (at l_o = const) leads to even more intensive oxidation of PQH_2. Interestingly, all $PQ(r)$ profiles calculated for the different values of geometric parameters l_o and l_i were similar to each other, in contrast to the lateral pH profiles.

The stationary lateral profiles of oxidized plastocyanin ([*Pc*]) are shown in Fig. 3b. The calculations showed that the shape of the profile of this mobile electron carrier was only weakly dependent on the variation of the geometric parameters and virtually identical for the metabolic states 3 and 4. However, an increase in l_o promoted a definite increase in the concentration of oxidized plastocyanin, whereas an increase in l_i promoted a decrease of local Pc concentration. This behavior can be explained if the rather long distances of plastocyanin diffusion in the luminal space (~100 nm) upon the transfer of electrons between the granal and stromal regions in the thylakoids are taken into account. The lumen width in a native chloroplast is comparable to the size of a plastocyanin molecule; therefore, plastocyanin diffusion is hindered considerably by the protruding parts of the transmembrane multi-enzyme complexes, and the rates of diffusion and electron transport depend on the lumen width, diffusion distance, and the structure of the luminal space. Continuous illumination of chloroplasts induces the swelling of these organelles; the drift of plastocyanin and its convergence with b_6f-complexes for electron transfer is thus facilitated.

CONCLUSIONS

Numerical experiments were performed with a model of the light stage of photosynthesis with the diffusion-controlled stages of electron and proton transport in the spatially inhomogeneous chloroplast taken into account. The results of these experiments showed that the model could serve as one of the tools for research on the effects of diffusion and steric restrictions on the distribution of pH and the behavior of mobile electron carriers (plastoquinone and plastocyanin) along the thylakoid membrane. The model enables the analysis of the effects of topological factors (spatial organization of thylakoids) on the rate of electron and proton transport and the synthesis of ATP in chloroplasts. The model predicted that inhomogeneous pH profiles could be established in granal and intergranal thylakoids of chloroplasts. The lateral profiles of pH_i and pH_o depended on the metabolic state of the chloroplasts, the degree of compaction of granal thylakoids, and the dimensions of the intrathylakoid space. Limited lateral mobility of protons can be due to the high density of proteins in the intrathylakoid space and the presence of a large number of buffer groups of proteins and lipids exposed on the inner surface of the thylakoids and in the interthylakoid gap. Processes of repeated proton binding to proton acceptor groups and dissociation from these groups ($B^- + H^+ \leftrightarrow BH$) can cause a decrease of the effective proton diffusion constant by several orders of magnitude [24, 25]. The lateral heterogeneity of the thylakoid membranes accounts for spatial separation of the majority of proton pumps (PS2 and cytochrome b_6f-complexes) and ATP synthase complexes related to the establishment of inhomogeneous pH_i profiles under the conditions of intense ATP synthesis (metabolic state 3). Experimental evidence in favor of this assumption was presented in several reports [2, 16, 17, 26]. The degree of granal thylakoid acidification decreases as the barriers for the lateral diffusion of protons are attenuated; this promotes a more homogeneous appearance of the lateral pH_i profiles. The lateral pH_i profiles are completely homogeneous in the state of photosynthetic control (state 4), when the leakage of protons through ATP synthase complexes does not occur.

Our calculations showed that variation of the topological factors of the lamellar system could exert a significant effect on the spatial distribution of pH along the thylakoid membrane and the redox state of mobile electron transporters (plastoquinone and plastocyanin). An increase of the model parameter l_i can be interpreted as the swelling of thylakoids upon illumination and an increase of l_o can be interpreted as the detachment of granal thylakoids from each other and the widening of the interthylakoid gap. Variation of the geometric dimensions of the thylakoids and the packing density of thylakoids in grana has a considerable effect on the lateral pH profiles. The pH_i decrease becomes more pronounced and the concentration of oxidized plastoquinone decreases as the width of the interthylakoid gap l_o increases. Conversely, acidification of the lumen becomes less pronounced and the concentration of oxidized plastoquinone increases as the width of the intrathylakoid space l_i increases. The results of numerical experiments that involved variation of the geometric parameters of the system provided an explanation for the results of earlier studies that revealed the dependence of the rate of ATP synthesis on the conditions of chloroplast incubation [26–29].

As a conclusion, let us emphasize that the results of calculations for the stationary states of chloroplasts are reported in the present study. The kinetics of the processes of proton and electron transport, as well as the dynamic aspects of the influence of topological factors on the functioning of the photosynthetic apparatus of

chloroplasts related to the light-induced changes in the geometric characteristics of chloroplasts (swelling or compaction of thylakoids [30]), will be addressed in our next report.

ACKNOWLEDGMENTS

The present work was supported by the Russian Foundation for Basic Research (grant no. 15-04-48981).

REFERENCES

1. G. Edwards and D. Walker, *C_3, C_4: Mechanisms, Cellular and Environmental Regulation of Photosynthesis* (Univ. of California Press, 1983).
2. L. A. Blumenfeld and A. N. Tikhonov, *Biophysical Thermodynamics of Intracellular Processes. Molecular Machines of the Living Cell* (Springer, New York, 1994).
3. R. E. Blankenship, *Molecular Mechanisms of Photosynthesis* (Blackwell, Maiden, 2002).
4. D. G. Nickolls and S. J. Ferguson, *Bioenergetics*, 3rd ed. (Academic Press, New York, 2002).
5. D. L. Nelson and M. Cox, *Lehninger Principles of Biochemistry*, 4th ed. (W. H. Freeman, New York, 2005), Chap. 20.
6. V. P. Skulachev, A. B. Bogachev, and F. O. Kasparinskii, *Membrane Bioenergetics. Textbook* (Mosk. Gos. Univ., Moscow, 2010).
7. A. B. Rubin and V. P. Shinkarev, *Electron Transport in Biological Systems* (Nauka, Moscow, 1984).
8. A. K. Kukushkin and A. N. Tikhonov, *Lectures on Biophysics of Photosynthesis of Higher Plants* (Mosk. Gos. Univ., Moscow, 1988).
9. H. Kirchhoff, S. Horstmann, and E. Weis, Biochim. Biophys. Acta **1459**, 148 (2000).
10. V. A. Karavaev and A. K. Kukushkin, Biofizika **38**, 958 (1993).
11. A. Rubin and G. Riznichenko, *Mathematical Biophysics* (Springer, 2014).
12. A. N. Tikhonov and A. V. Vershubskii, BioSystems **121**, 1 (2014).
13. P.-A. Albertsson, Trends Plant Sci. **6**, 349 (2001).
14. M. R. Badger and G. D. Price, J. Exp. Bot. **54**, 609 (2003).
15. A. N. Tikhonov, Plant Physiol. Biochem. **81**, 163 (2014).
16. A. N. Tikhonov and L. A. Blyumenfeld, Biofizika **30**, 527 (1985).
17. F. Haraux, Physiol. Veg. **23**, 397 (1985).
18. A. V. Vershubskii, V. I. Priklonskii, and A. N. Tikhonov, Biol. Membr. **20**, 184 (2003).
19. A. V. Vershubskii, V. I. Priklonskii, and A. N. Tikhonov, Biophysics **49**, 52 (2004).
20. A. V. Vershubskii, V. I. Priklonskii, and A. N. Tikhonov, Khim. Fiz. **26**, 54 (2007).
21. A. V. Vershubskii, I. V. Kuvykin, V. I. Priklonsky, and A. N. Tikhonov, Biosystems **103**, 164 (2011).
22. A. V. Vershubskii and A. N. Tikhonov, Biophysics **58**, 60 (2013).
23. J. Allen and J. Fosberg, Trends Plant Sci. **6**, 317 (2001).
24. W. Junge and A. Polle, Biochim. Biophys. Acta **848**, 265 (1986).
25. A. Polle and W. Junge, Biophys. J. **56**, 27 (1989).
26. Y. de Kouchkovsky, F. Haraux, and C. Sigalat, FEBS Lett. **139**, 245 (1982).
27. F. Haraux, C. Sigalat, A. Moreau, and Y. de Kouchkovsky, FEBS Lett. **155**, 248 (1983).
28. M. Masarova and A. N. Tikhonov, Biofizika **34**, 142 (1989).
29. M. Renganathan, R. S. Pan, R. G. Ewy, et al., Biochim. Biophys. Acta **1059**, 16 (1991).
30. H. Kirchhoff, Biochim. Biophys. Acta **1837**, 495 (2014).

Translated by S. Semenova